

1 of 1

APPENDIX A

DOE/ISF/18862-72-App.A
CONF-9307127-1-App.ANINTH TARGET FABRICATION SPECIALISTS MEETING
JULY 6-8, 1993 MONTEREY, CA

NEW POLYMER TARGET-SHELL PROPERTIES AND CHARACTERIZATIONS*

A. Honig, X. Wei, Q. Fan, N. Alexander and N. Palmer
Physics Dept., Syracuse Univ., Syracuse, NY 13244ABSTRACT

A method for characterizing ICF target shells is presented, based on measurement of the gas released from a single shell into a small volume. It utilizes cryogenic permeation systems developed in connection with our work on ICF targets containing nuclear spin-polarized D. Permeation rates for polystyrene and parylene-coated-polystyrene shells are measured at temperatures from 350K down to 180K. Burst or implosion pressure can be determined over a full temperature range down to 20K. Shell temperature is calculated from its gas leakage rate, calibrated by permeation measurements over the temperature range. Lag of shell temperature compared with sample-chamber temperature during warming of the latter is attributed to the weakness of the thermal link provided by both radiative heat transfer and free molecular conduction with small accommodation coefficients for helium and deuterium gas at the structure to which the shell is conductively linked, or at the surface of a conductively isolated shell. Quantification of this lag can provide a measure of atomic scale roughness of the shell outer surface. Also presented are reversible pre-rupture leakage phenomena for polystyrene and parylene-coated-polystyrene shells.

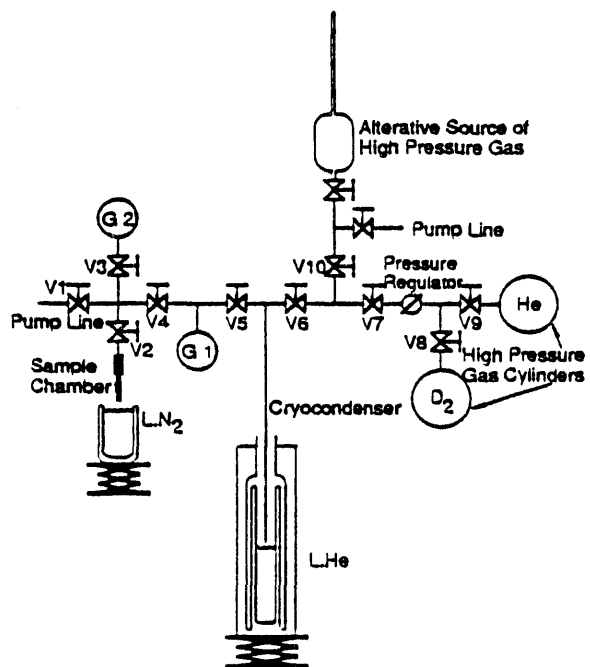


Fig. 1. Apparatus for permeation and burst pressure characterization of single polymer shells. High pressure gas is delivered to sample chamber either from gas cylinders or from cryocondenser. Shell inside sample chamber is filled to pressure $p_0(T_s)$, with T_s usually at room temperature, by incremental permeations. Temperature, T_c , of sample chamber, is then lowered by immersion in bath ($77K < T_c < 300K$). After reaching thermal equilibrium, sample chamber is rapidly evacuated and sealed from pump. Sample chamber pressure, P , monitored by Baratron (G2), increases from combination of background outgassing at rate b , and permeation from shell at a rate determined by the permeation coefficient for the material, $K_p(T_s)$, and the shell geometry. P' ($= P - bt$) is the background corrected pressure. Permeation constants are obtained in a constant T_s mode. Variable T_s experiments, consisting of slowly warming a shell initially at 77K by means of the weak thermal link to the sample chamber walls which are at held at high temperature, give shell burst pressures. A conceptually similar apparatus exists for experiments down to 4K.

*Work supported by DOE through LLNL Contract #B15736 and NLUF Grant #DE-FG03-91SF18862.

Target shells provided by R. Q. Gram and H. Kim of LLE, University of Rochester

FG03-91SF18862

MASTER

Fig. 2. PERMEATION OF SPHERICAL SHELL OF RADIUS r . W = wall thickness; T_s = shell temperature. Initial shell pressure = $p_0(T_s)$. Shell is inside sample chamber whose initial pressure is $P = 0$. ($P \ll p$ for more than 10 time constants since shell volume $V \ll$ sample chamber + Baratron volume, V). R is gas constant. K_p is permeation coefficient, with activation temperature α .

$$1. p_t(T_s) = p_0(T_s) e^{-\frac{t}{\tau}} \quad (\text{Shell pressure})$$

$$2. P = P - bt \quad (\text{Background corrected})$$

$$3. P' = P_f(1 - e^{-\frac{t}{\tau}}).$$

$$4. \tau = \frac{Wr}{3K_pRT_s}$$

$$5. K_p(T_s) = K_p(293) e^{-\alpha(\frac{1}{T_s} - \frac{1}{293})}$$

$$6. \tau(T_s) = \frac{\tau(293)}{T_s} e^{-\alpha(\frac{1}{T_s} - \frac{1}{293})}$$

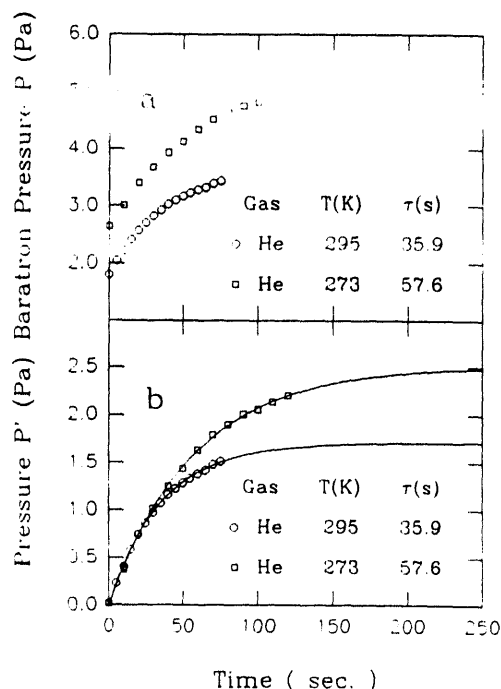


Fig. 3. Outgassing measurement of shell C, for determination of its permeation time-constant. a) P vs t ; b) P' vs t . Polystyrene shell, $r = 266 \mu\text{m}$, $W = 6 \mu\text{m}$, is loose in a screened aluminum cage. Similar results are obtained with a shell epoxied to a copper stalk.

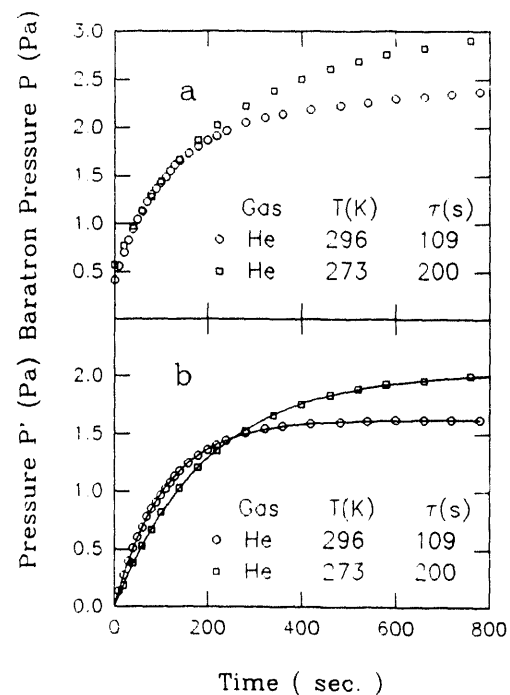


Fig. 4. Outgassing of shell E, to determine its permeation time-constant. a) P vs t ; b) P' vs t . Parylene-coated-polystyrene shell, $r = 265 \mu\text{m}$, $W_{\text{poly}} = 5 \mu\text{m}$, $W_{\text{par}} = 2 \mu\text{m}$, lies in a screened aluminum cage.

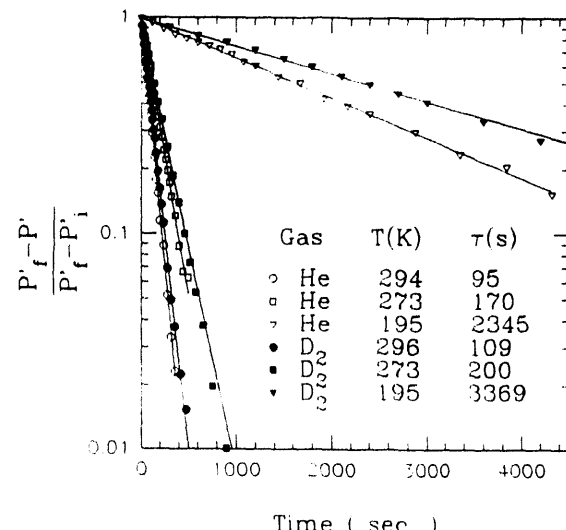


Fig. 5. Semi-logarithmic plot of $(P_f' - P') / (P_f' - P_i')$ vs time, whose slopes yield the time-constants for 2 gases at several temperatures for shell E.

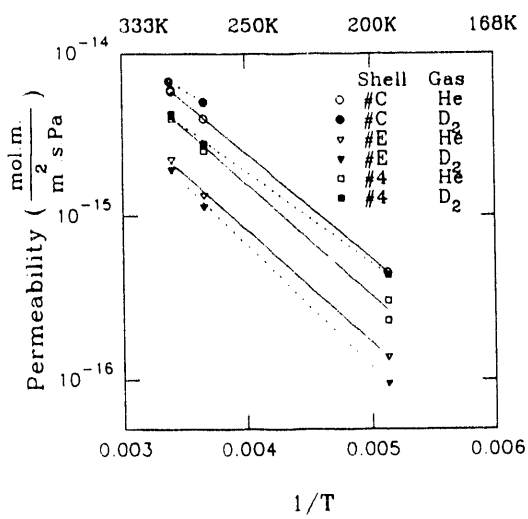


Fig. 6. Semi-logarithmic plot of permeability constant, K_p , vs reciprocal temperature. The slopes give α , the activation temperature, for the shells and gases used.

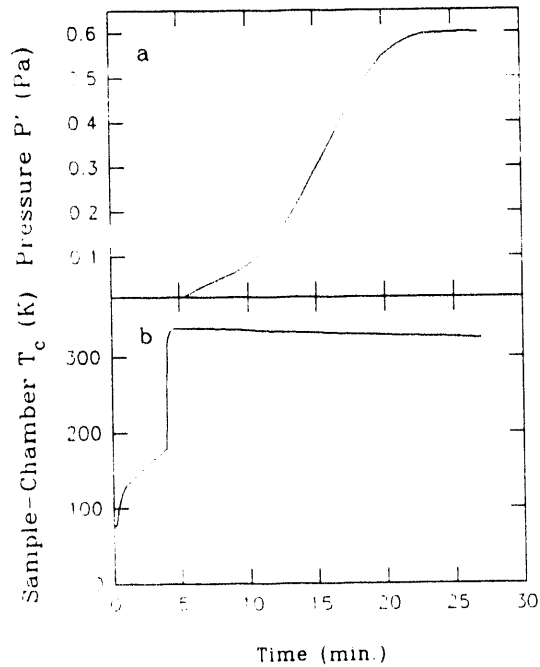


Fig. 7. P' and sample-chamber time profiles for shell E filled to 1 atm helium. a) P' vs t ; b) sample-chamber temperature vs t . At $t = 0$, liquid N_2 bath is removed from sample-chamber, and at $t = 4.0$ min, sample chamber is immersed in water at $T = 70^\circ C$.

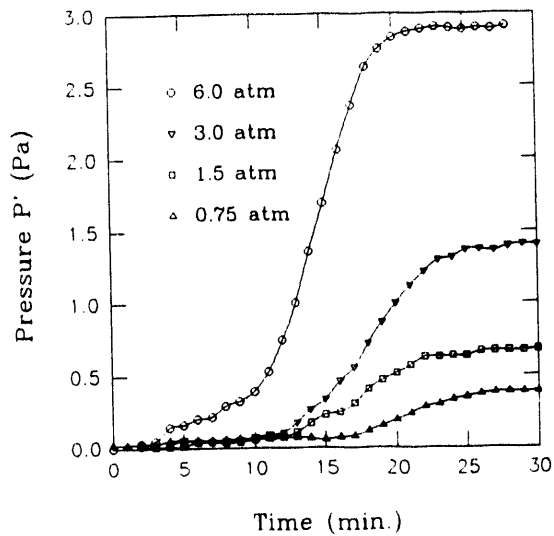


Fig. 8. P' vs t for shell E filled to four different pressures. Sample-chamber temperature profile is the same as described in caption of Fig. 7. Initial delay in pressure rise is during radiation-induced warm-up period. As temperature rises, outgassing commences. Faster relative out-gassing for higher fill-pressures shows pressure dependence of gas heat conduction.

Fig. 9. RADIATIVE AND GAS MOLECULAR CONDUCTION WARMING OF CONDUCTIVELY ISOLATED SHELL.

$$Q_S(RAD) = e_S \sigma A_S (T_C^4 - T_S^4),$$

$$Q_S(GAS) = \alpha_S \Lambda_O A_S \sqrt{\frac{273}{T_S}} (T_C - T_S) P,$$

where Q_S 's are in watts, P is measured in Pa,

α_S is the accommodation coefficient and

Λ_O is the free molecular conductivity:

$3.4 \times 10^{-4} \text{ w/cm}^2 \text{ }^\circ\text{C} \cdot \text{Pa}$ for deuterium,
 $2.3 \times 10^{-4} \text{ w/cm}^2 \text{ }^\circ\text{C} \cdot \text{Pa}$ for helium.

When shell is conductively linked to a conductively isolated (from sample chamber) support-structure, such as a stalk, or cage, subscripts s apply to support-structure rather than shell.

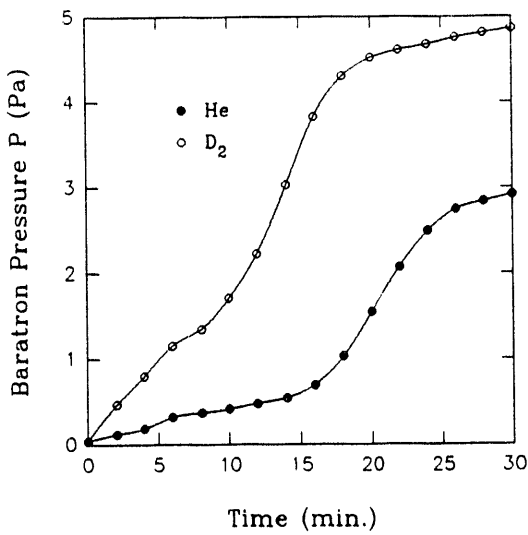


Fig. 10. P vs t for polystyrene shell #4, epoxied on copper stalk. $r = 288 \mu\text{m}$, $W = 10 \mu\text{m}$. Shell is filled to 6 atm with helium and with deuterium gas. Sample-chamber temperature profile is described in caption of Fig. 7. Shell filled with D_2 outgasses earlier than one filled with helium because of higher background outgassing rate of D_2 and larger accommodation coefficient on copper stalk of D_2 .

Fig. 11. SHELL TEMPERATURE MEASUREMENT FROM SHELL OUTGASSING RATE

1. Rate of outgassing depends on $\tau(T_s)$ and

pressure difference, $P_f^i - P_i^i$.

$$2. \left(\frac{dP}{dt} \right)_{P_i^i} = \frac{P_f^i - P_i^i}{\tau} = P_o \frac{v}{V} - P_i^i$$

$$3. \tau = \frac{P_o \frac{v}{V} - P_i^i}{\left(\frac{dP}{dt} \right)_{P_i^i}}$$

v and V are defined in Fig. 2. From the instantaneous τ values, T_s is inferred from the permeability determinations of Fig. 6 and Eq. 4 of Fig. 2.

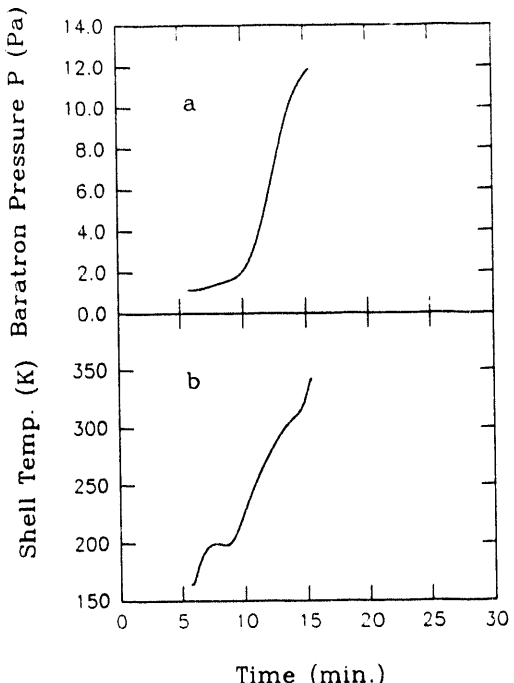


Fig. 12. a) P vs t ; b) Dduced temperature of shell E vs t , from Eq. 3 of Fig. 11. Temperature "plateau" in time interval near 8 min is believed due to start of cooling of shell via incipient gas conduction to cage, countering direct radiative warming of shell from walls of sample chamber.

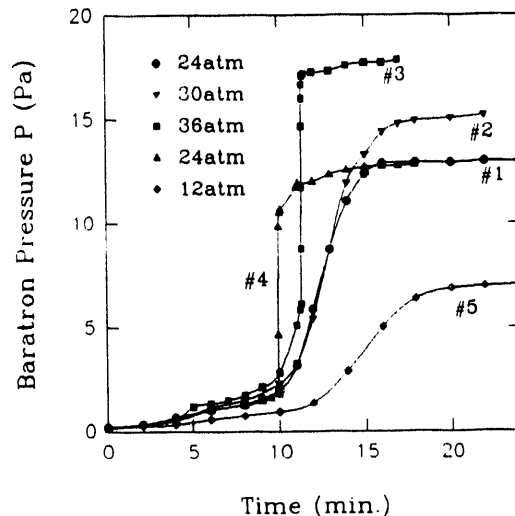


Fig. 13. P vs t for a series of shell E (parlylene coated polystyrene) fillings at higher pressures. Numbers alongside curves identify the order in which measurements were taken. Sample-chamber temperature profile is described in caption of Fig. 7 for all measurements in the series. Reversible damage (pre-rupture) is incurred in run #3, at a shell pressure of 18 atm, calculated from the T_s of the shell at the break point, and the gas leakage up to that point. It is noteworthy that the shell behaves entirely normally when refilled later to only 12 atm (fill #5).

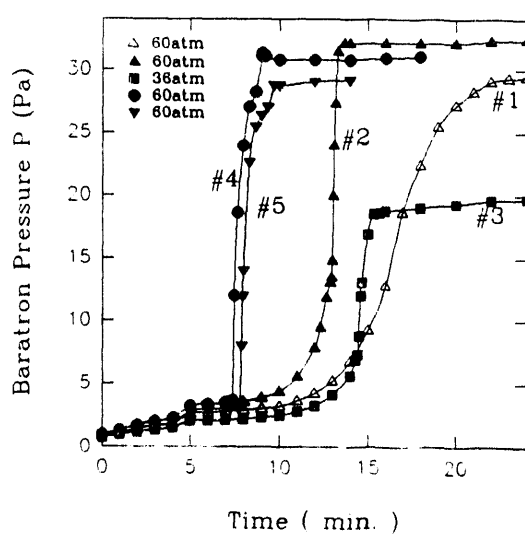


Fig. 14. P vs t for a series of helium gas fillings at higher pressures, for stalk-mounted polystyrene shell #3, $r = 262 \mu\text{m}$, $W = 9 \mu\text{m}$. Numbers alongside curves identify the order in which measurements were taken. Sample-chamber temperature profile is described in caption of Fig. 7 for all measurements in the series except for #1, where at $t = 4.0$ min, the sample-chamber temperature was raised to 40°C instead of the usual 70°C . The resultant slower radiative warming in #1 produced a normal outgassing, despite the high fill pressure. The faster warming rate in #2 resulted in "pre-rupture", similar to that in the previous figure, at a calculated pressure of 18 atm, with T_s at 235K. It is seen that the damage is not total, since the shell retains gas in subsequent cycles (#3 to #5). One notes that due to the gas law and the outgassing of a shell under these temperature-rise conditions, the internal shell pressure, p , rises from its

starting value at 77K of $\frac{77}{300} P_0$ over a considerable range, reaches a maximum, and then falls. If during this process the pressure exceeds $p(\text{burst})$, given by $2W\mathcal{J}(T_s)/r$, where $\mathcal{J}(T_s)$ is the temperature-dependent tensile strength, the shell explodes. Following an initial fill to 48 atmospheres, we did explode shell C at a pressure of 29 atmospheres, with T_s at 220K. This gives a $\mathcal{J}(220\text{K})$ of $61 \times 10^6 \text{ N/m}^2$, to be compared with the room temperature value, $48 \times 10^6 \text{ N/m}^2$. This is consistent with the increase of \mathcal{J} in other polymers with decreasing temperature. This method is convenient for measuring polymer tensile strength vs temperature, avoiding laborious experiments with incremental pressure increases for a measurement at a single temperature.

Fig. 15. SUMMARY

- 1.-Simple single shell K_p measurements. If shell is uniform and of known material, gives wall thickness.
- 2.-Temperature measurement of conductively isolated shell, or shell thermally-linked to a conductively isolated stalk.
- 3.-Simple burst pressure measurements as function of shell temperature.
- 4.-New "pre-rupture" shell phenomena.
- 5.-Emissivity and accommodation coefficient measurements of shell or supporting stalk.
- 6.-Use of measured accommodation coefficient at shell surface as a determinant of surface roughness on an atomic scale.
- 7.-Possibility of spatially profiling shell's surface roughness, thereby "tuning" the accommodation coefficient for a selected thermal gradient along the shell when there is uniform internal heat generation in the shell and rarefied (molecular conduction heat transfer regime) isothermal helium gas is the coolant.

The image consists of three rows of abstract black and white shapes. The top row contains four vertical rectangles of varying widths, arranged in a staggered pattern. The middle row features a large, solid black horizontal rectangle at the top, and below it, a large, solid black shape that tapers to a point and then extends diagonally downwards and to the right. The bottom row shows a large, solid black U-shaped cutout, with a white shape inside it that has a small dark speck in the center.

4154

DATA

